



Specific enrichment of urinary exosomes and exosomal glycopeptides by coefficient affinity of integrated L-cysteine and titania

Yijie Chen^a, Haolin Chen^a, Chenjie Yang^a, Yonglei Wu^a, Chunhui Deng^{a,b,*}, Nianrong Sun^{b,*}

^aDepartment of Chemistry, Institute of Metabolism & Integrate Biology (IMIB), Fudan University, Shanghai 200433, China

^bDepartment of Gastroenterology and Hepatology, Zhongshan Hospital, Fudan University, Shanghai 200032, China

ARTICLE INFO

Article history:

Received 25 November 2021

Revised 17 February 2022

Accepted 16 March 2022

Available online 19 March 2022

Keywords:

Glycopeptides

Enrichment

Nanomaterials

Exosomes

Urine

ABSTRACT

Exosome and inclusive cargoes have manifested significant function in different biological events. In particular, glycopeptides in exosome are closely associated with occurrence and development of various diseases. Developing advanced tools is highly desired to enrich glycopeptides from exosomes, and enrich exosomes from complex biological samples as well. In this work, integration of L-cysteine and titania onto the surface of magnetic nanoparticles is designed to realize the coefficient affinity towards exosomes and inclusive glycopeptides. Benefiting from the synergistic affinity, we separate exosomes from human urine concentrate directly, which was proved by the detection of three typical antigen markers of exosomes. Furthermore, hardly any exosomes remained on materials after ultrasonication, which confirmed the good capture performance of Fe₃O₄@TiO₂@L-Cys and high release effect of direct lysis. Moreover, 146 glycopeptides corresponding to 77 glycoproteins were successfully identified from captured exosomes. These satisfactory results will inspire more efforts to be devoted to this field and will be extremely helpful to in-depth information excavation of biological markers, especially disease-related ones, through exosomes and inclusive glycopeptides.

© 2022 Published by Elsevier B.V. on behalf of Chinese Chemical Society and Institute of Materia Medica, Chinese Academy of Medical Sciences.

It is well known that protein glycosylation is a kind of most vital post-translational modification (PTM) process [1,2], which plays an important role in numerous biological processes, such as cell signaling [3,4], proliferation [5], protein secretion [6] and tumor immunology [3,7]. Abnormal glycosylation is closely related to occurrence and development of diseases, especially evolution and progression in tumor [2,3,7–9]. Therefore, glycosylation research is significant that it can provide much information on differences of disease-associated glycoforms, or obtain a better understanding of the disease mechanism for early diagnosis [10–13]. In addition, body fluids such as blood, serum, saliva, breast milk and urine are the easiest access for diagnostic and therapeutic purpose [6,14–16]. Exosomes, as an important liquid biopsy target, were widely presented in various body fluids and tissues and contained many cargoes including glycoproteins [16–21]. Therefore, studies on exosomes and inclusive glycoproteins will be an effective way to monitor and analyze the physiological and pathological conditions.

However, challenges such as the complexity of biological samples and the relative low abundance of exosomes make it difficult to directly analyze exosomes and exosomal glycoproteins [22–25]. Therefore, it's necessary to conduct efficient enrichment process on a larger scale [17]. On account of the interaction between phospholipid bilayer membrane and titanium oxide, the excellent separation performance of titanium oxide towards exosomes in human urine was reported in a high-efficient and non-disruptive way [17,26,27]. Up to now, various strategies (hydrazide chemistry [6,28], boronic acid chemistry [29–31], lectin affinity chromatography [32], hydrophilic interaction chromatography (HILIC) [25,33,34], etc.) have been developed for enrichment of glycopeptides prior to MS identification. Therein, boronic acid methods are not favorable in enriching low-abundance glycopeptides because of the weak interactions [35,36]. Lectins have inherent specificity so that each kind of lectin can only recognize a specific glycan structure, which makes it hard to find a single lectin or lectin-combination to enrich all glycopeptides [23]. Among the aforementioned methods, HILIC methods exhibit an outstanding ability in universal glycopeptide enrichment and have been the most common use [37,38]. In this work, a novel strategy was proposed to

* Corresponding authors.

E-mail addresses: chdeng@fudan.edu.cn (C. Deng), sunnianrong@fudan.edu.cn (N. Sun).

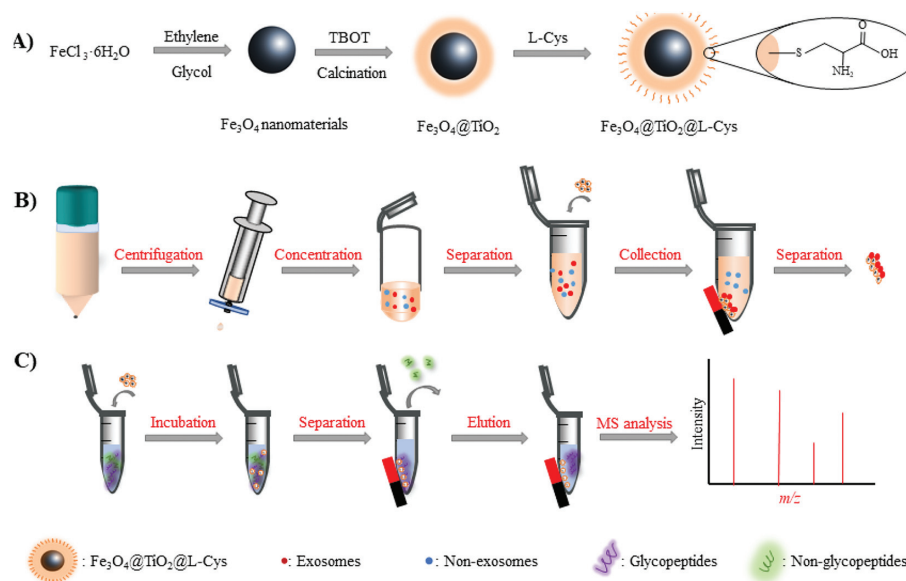


Fig. 1. Illustration of (A) the synthesis procedure of $\text{Fe}_3\text{O}_4@TiO_2@L\text{-Cys}$; (B) the urinary exosome purification process with $\text{Fe}_3\text{O}_4@TiO_2@L\text{-Cys}$; and (C) the glycopeptide enrichment procedure.

solve the difficulties in exosome separation and exosomal glycoprotein analysis.

L-cysteine (L-Cys) is a hydrophilic amino acid with superior biocompatibility and abundant polar groups such as amino, carboxyl and thiol. According to early reports, interaction between titanium and the thiol group remains L-Cys immobilized on TiO_2 [38,39]. Considering titanium oxide was an ideal functional unit with ability to separate exosomes by binding the phosphate group of the exosomal phospholipid bilayer [40,41], hence, we successfully integrated L-Cys and titania onto the surface of magnetic nanoparticles in a simple procedure (denoted as $\text{Fe}_3\text{O}_4@TiO_2@L\text{-Cys}$), by which the coefficient affinity towards exosomes and exosomal glycoproteins was achieved. In addition to the great enrichment performance for exosomes and glycoproteins, the $\text{Fe}_3\text{O}_4@TiO_2@L\text{-Cys}$ displayed strongly magnetic responsiveness, which made the separation process rapid and effortless under external magnetic field. Notably, the exosome lysis was directly implemented after the exosomes were captured by $\text{Fe}_3\text{O}_4@TiO_2@L\text{-Cys}$ from human urine samples without extra elution process. Afterwards, the difunctional material was employed to enrich glycopeptides from these urinary exosomes based on hydrophilic interactions followed by LC-MS/MS analysis.

The synthetic process of $\text{Fe}_3\text{O}_4@TiO_2@L\text{-Cys}$ is manifested in Fig. 1A. Transmission electron microscopy (TEM) was applied to characterize this dual-functional material. It is clear in Fig. 2A that the boundaries of Fe_3O_4 were surrounded by agminated nanoparticles after modified by TiO_2 and L-Cys. The diameter of Fe_3O_4 core was about 200 nm, and increased to approximately 300 nm after modification, which reveals the diameter of TiO_2 and L-Cys shell was around 100 nm. TiO_2 was utilized to form a protective shell, making this magnetic material a favorable substrate for exosome capture and further modification of hydrophilic groups. The ζ potential parameters under neutral condition were measured to monitor the synthetic process as demonstrated in Fig. 2B. It's clear that the ζ potential changed along with the progress of modification procedure. In detail, the ζ potential of Fe_3O_4 was recognized as 4.03 mV. After coated with TiO_2 and L-Cys layer upon layer, the value gradually decreases to minus.

The energy dispersive X-ray (EDX) spectrum for element detection was shown in Supporting information (Fig. S1 in Supporting information), distinctly displaying that C, O, N, Fe, S and Ti

elements are homogeneously distributed, implying the successful modification of TiO_2 and L-cysteine. Furthermore, Fourier transform infrared (FTIR) spectroscopy was applied to characterize functional groups on $\text{Fe}_3\text{O}_4@TiO_2@L\text{-Cys}$. As shown in Fig. 2C, typical adsorption peak at 585 cm^{-1} was ascribed to Fe-O stretching vibration in FTIR spectra [42,43]. Various peaks between 400 cm^{-1} and 1400 cm^{-1} and 2525 cm^{-1} vibration in fingerprint region were all attributed to the characteristic peaks in L-Cys [44]. Other broad absorption bands at 1667 , 1585 , 1340 cm^{-1} were assigned to the stretching modes of COOH, NH_2 and CH groups, respectively [45]. This information further confirmed the successful modification of L-Cys. Moreover, the amount of L-Cys modified on $\text{Fe}_3\text{O}_4@TiO_2$ nanoparticles was also compared as illustrated in Fig. S2 (Supporting information). The material performed best when the ratio of $\text{Fe}_3\text{O}_4@TiO_2$ to L-Cys was 1:3.

The magnetic response, dispersity in aqueous solution and hydrophilicity of $\text{Fe}_3\text{O}_4@TiO_2@L\text{-Cys}$ were tested respectively. The results showed the saturated magnetic value of $\text{Fe}_3\text{O}_4@TiO_2@L\text{-Cys}$ was 44.31 emu/g (Fig. 2D), which was capable of conducting magnetic separation [18,41]. As observed in Fig. 2E, the dispersed $\text{Fe}_3\text{O}_4@TiO_2@L\text{-Cys}$ can be separated from aqueous solution within 5 s using a magnet. Water contact angle test was conducted to prove the hydrophilicity of $\text{Fe}_3\text{O}_4@TiO_2@L\text{-Cys}$. The water contact angle gradually decreased from 45.06° to 25.04° , and then to 20.47° after successive modification by TiO_2 and L-Cys (Fig. 2F), indicating the introduction of titania shell and L-Cys can improve the hydrophilicity of Fe_3O_4 , which will contribute to glycopeptide capture based on hydrophilic interaction. All above characterizations proved the successful synthesis and excellent properties of $\text{Fe}_3\text{O}_4@TiO_2@L\text{-Cys}$. The TiO_2 functionalized surface and hydrophilic exterior surface would contribute to intact exosome capture and glycopeptide enrichment.

As a proof of coefficient enrichment strategy based on $\text{Fe}_3\text{O}_4@TiO_2@L\text{-Cys}$, the ability for exosome capture was demonstrated by using urine concentrate of human volunteers as sample. The urinary exosome purification process was manifested in Fig. 1B. Western blotting results confirmed the presence of three typical antigen markers of exosomes (TSG101, CD63, CD9) which were commonly expressed on the exosome surface (Fig. S3 in Supporting information), revealing the selective exosome capture ability of this difunctional material. These material-captured exosomes were

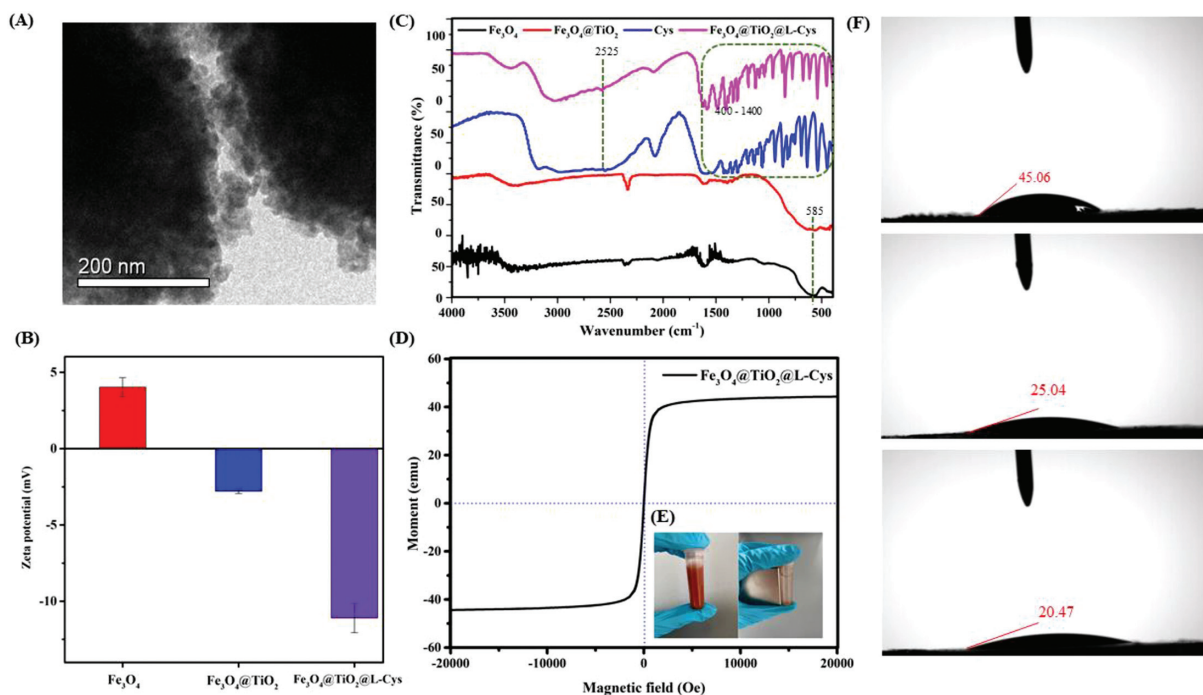


Fig. 2. Characteristic of $\text{Fe}_3\text{O}_4@TiO_2@L-Cys$. (A) TEM images, (B) ζ potential of Fe_3O_4 , $\text{Fe}_3\text{O}_4@TiO_2$ and $\text{Fe}_3\text{O}_4@TiO_2@L-Cys$, (C) FTIR spectroscopy of Fe_3O_4 , $\text{Fe}_3\text{O}_4@TiO_2$, L-Cys and $\text{Fe}_3\text{O}_4@TiO_2@L-Cys$. (D) Magnetic hysteresis loop $\text{Fe}_3\text{O}_4@TiO_2@L-Cys$, (E) $\text{Fe}_3\text{O}_4@TiO_2@L-Cys$ dispersed in aqueous solution and separated in 5 s via a magnet and (F) contact angles of Fe_3O_4 , $\text{Fe}_3\text{O}_4@TiO_2$ and $\text{Fe}_3\text{O}_4@TiO_2@L-Cys$.

lysed with the aid of ultrasound. After lysis, CD9 and TSG101 were invisible in images and the color of CD63 was also lighten, which indicated that the majority of exosomes were released from the materials after ultrasonication. These results confirmed the good capture performance of $\text{Fe}_3\text{O}_4@TiO_2@L-Cys$ and high release effect of direct lysis.

Another design of $\text{Fe}_3\text{O}_4@TiO_2@L-Cys$ was to analyze glycopeptides of exosomes further, and the glycopeptide enrichment procedure was shown in Fig. 1C. The capacity and specificity were primarily investigated by employing HRP as a standard glycoprotein. As shown in Fig. S2, the signals of glycopeptides were severely suppressed by abundant non-glycopeptides before enrichment when 100 fmol/ μL HRP digest was used as a model sample. However, after enrichment with $\text{Fe}_3\text{O}_4@TiO_2@L-Cys$, the interference was most eliminated. A total of 32 significant peaks corresponding to N-glycopeptides were identified (Figs. S4, S5 and Table S1 in Supporting information), demonstrating the excellent performance of $\text{Fe}_3\text{O}_4@TiO_2@L-Cys$ for enrichment of N-linked glycopeptides. Then the conditions of $\text{Fe}_3\text{O}_4@TiO_2@L-Cys$ for enrichment process were explored, mainly including incubation and elution condition, since it is well-known that the vital factor of HILIC-based materials in glycopeptides enrichment is the ratio of acetonitrile (ACN) to trifluoroacetic acid (TFA). Herein, different ratios of ACN and TFA in both loading buffer and eluting solution were explored for achieving the optimal performance [46–48]. After overall considering the number and intensity of identified glycopeptides, and background of interference of artifactual bands, the optimized enrichment parameters of ACN: H_2O :TFA were chosen as 95:4.9:0.1 and 50:49:1 as incubating and eluting solvent, respectively (Fig. 3 and Fig. S6 in Supporting information). Furthermore, the sensitivity and selectivity of $\text{Fe}_3\text{O}_4@TiO_2@L-Cys$ were assessed in view of the low abundance of glycopeptides in biological samples. The results indicated the sensitivity could be as low as 0.1 fmol/ μL (Fig. S7 in Supporting information), and the selectivity reached 1:100 (HRP/BSA, wt/wt, Fig. S8 in Supporting information), revealing high sensitivity and good anti-interference ability.

Next, to verify the successive effectiveness of $\text{Fe}_3\text{O}_4@TiO_2@L-Cys$ towards exosome capture and glycopeptide enrichment, we further applied this material to enrich glycopeptides from the aforementioned urine exosomes. A total of 146 glycopeptides corresponding to 77 glycoproteins were identified by nano-LC-MS/MS. Compared with the extraction of exosomes in other studies, separating procedure of exosomes in this work shortened the analysis time by effective binding of phosphate group on exosomes with titanium oxygen on material [18,49]. The detailed information of identified glycopeptides was listed in Table S2 (Supporting information). To combine the glycopeptides analysis with the correlated biological function, gene ontology (GO) analysis was conducted through the database for annotation visualization, integrated discovery database (DAVID) and a web platform for scientific data visualization (Hiplot, <https://hiplot.com.cn>). The results of GO analysis of the biological process of human volunteers in Fig. 4 showed that the identified exosomal glycopeptides were mainly related to platelet degranulation, proteolysis and receptor-mediated endocytosis, and most glycopeptides were inclined to be localized at the extracellular exosome and extracellular space, which were generally consistent with early reports [50]. Glycopeptides were mainly involved in immunoglobulin receptor binding, dipeptidyl-peptidase activity and peptide binding from the view of molecular function, which were also proved in early study [3,19,20]. In addition, the main KEGG (Kyoto encyclopedia of genes and genomes) pathways of glycoproteins from urinary exosomes were involved in lysosome and phagosome, which were related to the exosome internalization and release. These glycoproteins carried by urinary exosomes may play a significant role in cell activities, disclosing the potential of exosomal glycopeptides in promoting the progress of precision medicine initiatives.

In summary, a novel dual-functional magnetic nanomaterial $\text{Fe}_3\text{O}_4@TiO_2@L-Cys$ constructed in a facile and convenient one-pot approach was proposed. With the utilization of titanium oxide, good capture performance towards exosomes and high release effect after direct lysis were realized. This novel material with abun-

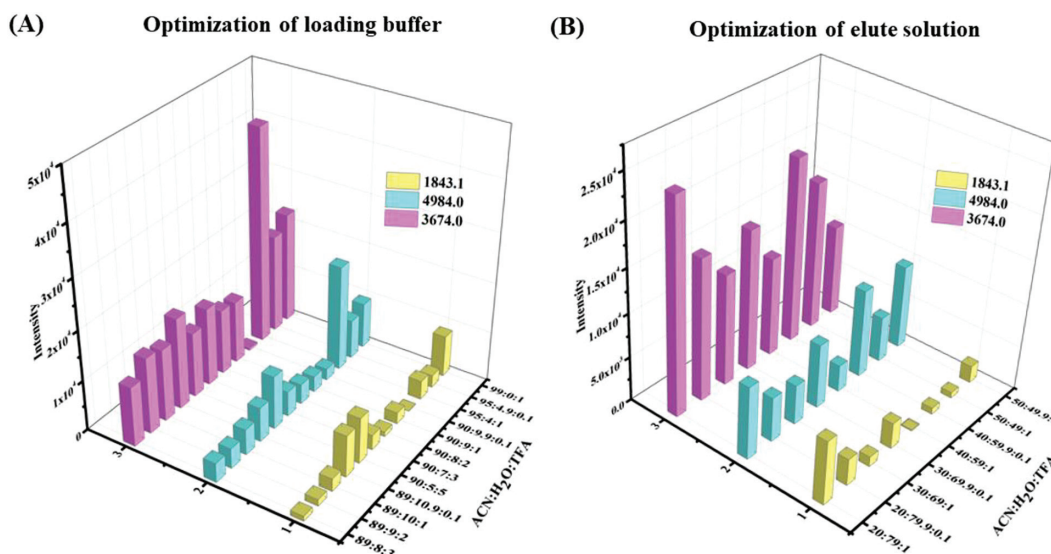


Fig. 3. Glycopeptide enrichment performance of $\text{Fe}_3\text{O}_4@TiO_2@L\text{-Cys}$. The intensity of three typical glycopeptides enriched from HRP tryptic digests using different ratios of ACN: H_2O :TFA in (A) loading buffer and (B) eluting solution.

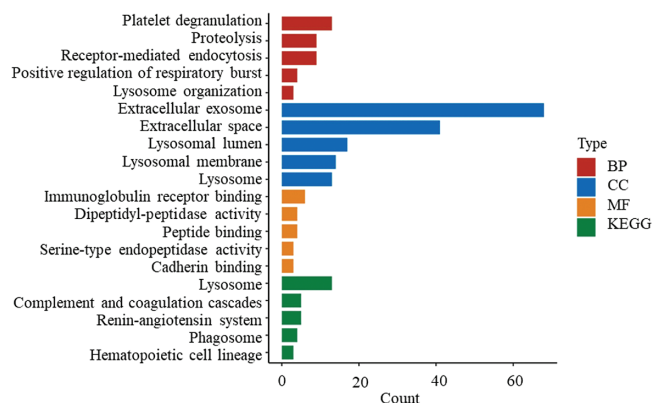


Fig. 4. The gene ontology (GO) and Kyoto encyclopedia of genes and genomes (KEGG) pathways of isolated urine exosomes. BP (biological process), CC (cellular components) and MF (molecular function) are three typical analyses of GO.

dant hydrophilic groups manifested high sensitivity and outstanding practical applicability in glycopeptide enrichment. A total of 146 glycopeptides corresponding to 77 glycoproteins were captured from human urine exosomes. Gene ontology and Kyoto encyclopedia of genes and genomes analysis all revealed that the identified exosomal glycoproteins exerted influence on diverse biological processes. These studies on exosome separation and glycoprotein analysis prove $\text{Fe}_3\text{O}_4@TiO_2@L\text{-Cys}$ to be a potent tool for exosomal glycoproteomics. However, only a small number of samples were used in this work, more samples should be conducted to provide a comprehensive understanding towards exosomes and the corresponding glycoproteome. More importantly, disease samples should be explored in future given the emerging of precise medicine area.

Declaration of competing interest

The authors declare no conflict of interest.

Acknowledgments

This work was supported by National Key R&D Program of China (No. 2018YFA0507501), the National Science Foundation for Distinguished Young Scholars of China (No. 21425518), the National

Natural Science Foundation of China (Nos. 22074019, 22004017), and Shanghai Sailing Program (No. 20YF1405300).

Supplementary materials

Supplementary material associated with this article can be found, in the online version, at doi:10.1016/j.ccl.2022.03.075.

References

- [1] R.G. Spiro, *Glycobiology* 12 (2002) 43R–56R.
- [2] D.F. Zielinska, F. Gnad, J.R. Wisniewski, M. Mann, *Cell* 141 (2010) 897–907.
- [3] K. Ohtsubo, J.D. Marth, *Cell* 126 (2006) 855–867.
- [4] Y. Li, J. Wang, N. Sun, C.H. Deng, *Anal. Chem.* 89 (2017) 11151–11158.
- [5] G. Qing, Q. Lu, Y. Xiong, et al., *Adv. Mater.* 29 (2017) 1604670.
- [6] H. Zhang, X.J. Li, D.B. Martin, R. Aebbersold, *Nat. Biotechnol.* 21 (2003) 660–666.
- [7] M.M. Fuster, J.D. Esko, *Nat. Rev. Cancer* 5 (2005) 526–542.
- [8] L. Zhu, J. Zhao, Z. Guo, et al., *Biosensors* 11 (2021) 344.
- [9] M. Liu, L. Xi, T. Tan, et al., *Chin. Chem. Lett.* 32 (2021) 1726–1730.
- [10] H.H. Freeze, E.A. Eklund, B.G. Ng, M.C. Patterson, *Lancet. Neurol.* 11 (2012) 453–466.
- [11] T. Hennet, *Biochim. Biophys. Acta* 1820 (2012) 1306–1317.
- [12] J. Yao, J. Wang, N. Sun, C. Deng, *Nanoscale* 9 (2017) 16024–16029.
- [13] Y. Tian, H. Zhang, *Proteom. Clin. Appl.* 4 (2010) 124–132.
- [14] J. Roth, *Chem. Rev.* 102 (2002) 285–303.
- [15] Z. Li, C. Hu, J. Jia, et al., *J. Biomed. Nanotechnol.* 15 (2019) 1090–1096.
- [16] X. Sun, Y. Wang, K. Gu, et al., *Mater. Express* 11 (2021) 46–53.
- [17] Y. Wu, N. Zhang, H. Wu, N. Sun, C. Deng, *Microchim. Acta* 188 (2021) 66.
- [18] S. Guan, H. Yu, G. Yan, et al., *J. Proteome Res.* 19 (2020) 2217–2225.
- [19] S.A. Melo, H. Sugimoto, J.T. O'Connell, et al., *Cancer Cell* 26 (2014) 707–721.
- [20] S.A. Melo, L.B. Luecke, C. Kahlert, et al., *Nature* 523 (2015) 177–182.
- [21] H. Zhang, Y. Lv, J. Du, et al., *Anal. Chim. Acta* 1098 (2020) 181–189.
- [22] J. Wang, J. Yao, N. Sun, C. Deng, *J. Chromatogr. A* 1512 (2017) 1–8.
- [23] H. Xiao, W. Chen, J.M. Smeekens, R. Wu, *Nat. Commun.* 9 (2018) 1692.
- [24] A. Chernykh, R. Kawahara, M. Thaysen-Andersen, *Biochem. Soc. Trans.* 49 (2021) 161–186.
- [25] G. Qing, J. Yan, X. He, X. Li, X. Liang, *Trends Analyt. Chem.* 124 (2020) 115570.
- [26] H. Dong, C. Tang, Z. He, et al., *Chin. Chem. Lett.* 31 (2020) 1812–1816.
- [27] Z. Li, C. Hu, J. Jia, et al., *J. Biomed. Nanotechnol.* 17 (2021) 407–415.
- [28] J. Wohlgenuth, M. Karas, T. Eichhorn, R. Hendriks, S. Andrecht, *Anal. Biochem.* 395 (2009) 178–188.
- [29] S. Kong, Q. Zhang, L. Yang, et al., *Anal. Chem.* 93 (2021) 6682–6691.
- [30] X.M. Wang, Z.J. Hu, P.F. Guo, M.L. Chen, J.H. Wang, *ACS Appl. Mater. Interfaces* 12 (2020) 43273–43280.
- [31] C. Zhang, X. Jin, L. Wang, et al., *ACS Appl. Mater. Interfaces* 13 (2021) 9714–9728.
- [32] J.C. Trinidad, R. Schoepfer, A.L. Burlingame, K.F. Medzihradszky, *Mol. Cell Proteomics* 12 (2013) 3474–3488.
- [33] S. Mysling, G. Palmisano, P. Hojrup, M.T. Andersen, *Anal. Chem.* 82 (2010) 5598–5609.
- [34] P. Hagglund, J. Bunkenborg, F. Elortza, O.N. Jensen, P. Roepstorff, *J. Proteome Res.* 3 (2004) 556–566.

- [35] L. Zhang, Y. Xu, H. Yao, et al., *Chemistry* 15 (2009) 10158–10166.
- [36] W. Chen, J.M. Smeekens, R. Wu, *Mol. Cell Proteomics* 13 (2014) 1563–1572.
- [37] Y. Wu, H. Lin, Z. Xu, et al., *Anal. Chim. Acta* 1096 (2020) 1–8.
- [38] N. Sun, Z. Wang, J. Wang, et al., *J. Chromatogr. A* 1595 (2019) 1–10.
- [39] N. Zhang, N. Sun, C. Deng, *Chem. Commun.* 56 (2020) 13999–14002.
- [40] N. Zhang, X. Hu, H. Chen, C. Deng, N. Sun, *Chem. Commun.* 57 (2021) 6249–6252.
- [41] H. Zheng, S. Guan, X. Wang, et al., *Anal. Chem.* 92 (2020) 9239–9246.
- [42] H. Chen, Y. Li, H. Wu, N. Sun, C. Deng, *ACS Sustain. Chem. Eng.* 7 (2019) 2844–2851.
- [43] H. Chu, X. Hu, J. Yao, et al., *Talanta* 206 (2020) 120178.
- [44] Y. Wu, Q. Liu, C. Deng, *Anal. Chim. Acta* 1061 (2019) 110–121.
- [45] X. Feng, C. Deng, M. Gao, X. Zhang, *Anal. Bioanal. Chem.* 410 (2018) 989–998.
- [46] W. Ma, L. Xu, X. Li, et al., *ACS Appl. Mater. Interfaces* 9 (2017) 19562–19568.
- [47] N. Sun, J. Wang, J. Yao, C. Deng, *Anal. Chem.* 89 (2017) 1764–1771.
- [48] Q. Liu, Y. Xie, C. Deng, Y. Li, *Talanta* 175 (2017) 477–482.
- [49] N. Zhang, N. Sun, C. Deng, *Talanta* 221 (2021) 121571.
- [50] Z. Xu, Y. Wu, Z. Deng, et al., *Talanta* 234 (2021) 122713.